Journal of Applied Polymer Science

Dielectric property, electric breakdown, and discharged energy density of a poly(vinylidene fluoride-co-chlorotrifluoroethylene) copolymer with low temperature processing

Weimin Xia,[1,2] Fan Liang,[1] Junhong Xing,[1] Zhuo Xu[2]

[1]Institute of Printing and Packaging Engineering, Xi'an University of Technology, Xi'an 710048, Shaanxi, China

[2]Electronic Materials Research Laboratory, Key Laboratory of the Ministry of Education, Xi'an Jiaotong University, Xi'an 710049, Shaanxi, China

Correspondence to: W. Xia (E-mail: xia.weimin@stu.xjtu.edu.cn)

ABSTRACT: Different thermal processing methods were used to fabricate the crystalline properties of poly(vinylidene fluoride-*co*-chlorotrifluoroethylene) [P(VDF-*co*-CTFE)] films. We observed that the crystallinity and crystal grain size of the various samples decreased with the quenching temperature. Compared to that of the annealed P(VDF-*co*-CTFE) sample, a higher dielectric constant of 13.9 at a frequency of 100 Hz was obtained in the film with liquid nitrogen quenching because the increasing small crystalline regions were susceptible to the excitation of external electric field. Meanwhile, the breakdown electric strength of the low-temperature-quenched film increased to 530 MV/m when the depth of shallow electronic energy level decreased, as depicted by Fröhlich collective electron approximated electric breakdown theory. Moreover, when we introduced the leakage current density curves, the effect of the space charges on the electric displacement was proven. As a result, the discharged energy density of the liquid-nitrogen-quenched P(VDF-*co*-CTFE) film was enhanced to 15.32 J/cm^3 at an electric field of 530 MV/m; this provided an effective way in addition to chemical modification to achieve a high energy storage ability in this poly(vinylidene fluoride)-based fluoropolymer. © 2015 Wiley Periodicals, Inc. J. Appl. Polym. Sci. **2015**, *132*, 42794.

KEYWORDS: copolymers; crystallization; properties and characterization

Received 14 September 2014; accepted 30 July 2015

DOI: 10.1002/app.42794

INTRODUCTION

With the increasing demands for high energy and power density capacitors for advanced dielectric applications, such as power conditioning, electric launch platforms, and electrical and hybrid vehicles, many researchers have put all of their efforts into seeking novel materials with favorable dielectric properties.[1–3] Compared to traditional dielectric ceramic, electrolytic, and mica for advanced capacitors, poly(vinylidene fluoride) (PVDF)-based fluoropolymers possess apparent advantages, including a high breakdown electric field (E_b), good mechanical elasticity, ease of film fabrication, low cost, and self-healing ability. After it is fabricated into films or blocks with various thicknesses, it shows favorable dielectric, ferroelectric, and piezoelectric properties because of its high polar C—F and C—C dipoles.[4] Recently, it was confirmed that the energy density of the PVDF-based copolymer poly(vinylidene fluoride-*co*-chlorotrifluoroethylene) [P(VDF-*co*-CTFE)] in the nonpolar α phase could reach 25 J/cm^3 under an electric field (E) of about 650 MV/m after it was stretched to a ratio of over 500%.[5–8] The author claimed that the existence of the Cl atom in the chlorotrifluoroethylene (CTFE) units stabilized the nonpolar α phase of the copolymer. In contrast to the phase transition from the α to the γ phase under 300 MV/m in pure PVDF, no phase transition was observed in the stretched P(VDF-*co*-CTFE) film even under a high electrical field.[9] In addition to mechanical stretching, the introduction of a certain molar content (ca. 8 mol %) of CTFE or chloridedifluoride ethylene into another PVDF-based copolymer, poly(vinylidene fluoride–trifluoroethylene), turned the crystal phase from the high polar β phase into the γ phase with medium polarity.[10–12] The E value of displacement saturation was improved to about 500 MV/m; this depended on the CTFE or chloridedifluoride ethylene composition, and the discharged energy density of the obtained terpolymer was as high as 13 J/cm^3.[13] Since then, many works about the energy storage properties of PVDF and its co(ter)polymers have been published,[14–17] and a great enhancement of over 20 J/cm^3 in the energy density has been achieved. However, the applied E could not be improved further because of the limitation of the displacement saturation, which was due to the intrinsic characteristics of the crystal phase in the PVDF-based polymers.

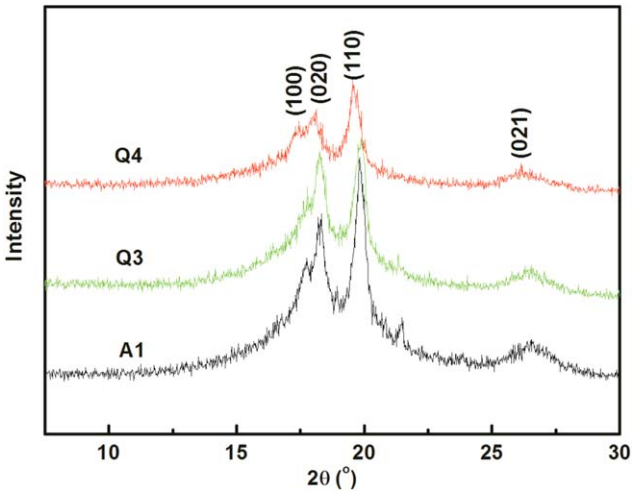

Figure 1. X-ray diffraction of the three quenched copolymers at room temperature. [Color figure can be viewed in the online issue, which is available at wileyonlinelibrary.com.]

It has been well reported that P(VDF-*co*-CTFE) is a nonlinear dielectric polymer whose discharged energy density can be calculated with the integral results of $U_e = \int EdD$ rather than those obtained directly from $U_e = 1/2\varepsilon_0\varepsilon_r E^2$,[15–17] where U_e is discharged energy density, ε_0 is dielectric permittivity of vacuum, and ε_r is the dielectric constant. This indicated that the large electric displacement (D) and E_b were the predominant issues for improving the energy storage ability.[18] Previous work has mostly concentrated on the molecular structure design and phase modification of PVDF-based polymers to enhance the value of D.[19–21] Less attention has been paid on how to improve their breakdown strength by revealing the electric breakdown mechanism of this polymer. According to the Fröhlich theory[22] and the related literature,[23] the electrical breakdown field of the polymer not only relies on its molecular structure (i.e., composition and monomer) but also fully depends on the condensed state (i.e., crystal size and crystallinity). Although the crystal property dependence of the discharged energy density of P(VDF-*co*-CTFE) with a 6% CTFE molar content was proposed in our former study,[24] the effects of conduction loss on the dielectric response and D were not included. Therefore, in this study, different P(VDF-*co*-CTFE) films with various crystalline properties were prepared via the fabrication of the same solution-cast films under different thermal conditions. Finally, by explaining the crystal property dependence of its electric breakdown strength, dielectric response, and D, we obtained a large discharged energy density in liquid-nitrogen-quenched P(VDF-*co*-CTFE) films.

EXPERIMENTAL

Preparation of the P(VDF-*co*-CTFE) Films

P(VDF-*co*-CTFE) powder was purchased from Solvay Solex Co., and the molar content of vinylidene fluoride units was 91%. After further purification, typical copolymer films were obtained with the following procedures. P(VDF-*co*-CTFE) was dissolved in dimethylformamide with a concentration about 5 wt % with continuous stirring with a magnetic stirrer for 3 h. The obtained solution was cast onto a quartz slide in an oven at 70°C with reduced pressure. Then, the preformed films were heated at 200°C (above its melting point of 160°C) in the oven for 30 min. To fabricate the P(VDF-*co*-CTFE) copolymers with different crystal properties, the melted films were annealed or quenched under various special conditions as follows. The films were annealed in the same oven at 140°C (marked as A1), cooled in air at room temperature (25°C; marked as Q1), quenched in an ice–water bath (0°C; marked as Q2), quenched in a hexane–liquid nitrogen bath (−94°C; marked as Q3), or quenched in liquid nitrogen (−195.8°C; marked as Q4), respectively. For electric characterization, a gold electrode (thickness = 80 nm, diameter = 2 mm) was sputtered on both surfaces of the polymer films with a JEOL JFC-1600 auto fine coater (Japan). The small electrode area was designed to prevent the influence of the defect and express the intrinsic electric properties of the P(VDF-*co*-CTFE) films.

Characterization

X-ray diffraction (Rigaku D/MAX-2400, Rigaku Industrial Corp., Japan) was performed to characterize the crystal structure and crystallinity of the P(VDF-*co*-CTFE) films, and the wavelength of the X-ray was 1.542 Å (Cu Kα radiation, 40 kV, 100 mA, and 10°/min). The crystallinity was also calculated with a differential scanning calorimeter (Netzsch TG209, Germany). A polarizable optical microscope (Olympus BX51-B, Japan) was used to observe the crystal grain size of the films. E_b was measured on a direct current with a voltage (V) tester. The dielectric properties were detected with an Agilent inductance-capacitance-resistance meter (LCR) meter (4294A and 4284). The D–E hysteresis loops and current (I)–V curves were obtained by a ferroelectric test system (TF Analyzer 2000, aixACCT, Germany).

RESULTS AND DISCUSSION

Crystalline Properties

It was confirmed that among the main crystal structures (α, β, γ, and δ) of PVDF,[5] the most kinetically α phase favored a high energy density. As shown in the X-ray diffraction presented in Figure 1, four major peaks at 17.1, 18.2, 19.9, and 26.8° of all of the samples corresponded to the (100), (020), (110), and (021) planes of the α phase; this indicated that low-temperature quenching had little influence on the crystal phase of P(VDF-*co*-CTFE).[25–27] However, the various X-ray diffraction peak strengths illustrated that A1, Q3, and Q4 possessed different crystalline properties,[28] as shown in Figure 1. According to the Sheller formula,[29,30] the broader peak and depressed diffraction intensity indicated that the crystallinity and crystal grain size decreased as the quenching temperature was decreased.

The depressed crystallinity in the low-temperature-quenched P(VDF-*co*-CTFE) was also illustrated by the differential scanning calorimetry curves. As shown in Figure 2, the V-shaped peak referred to the melting point. Apparently, the melting point of the sample decreased from 159.5°C (A1) to 154.1°C (Q4); this was attributed to the increasing amorphous phase in the low-temperature-quenched sample.[31,32] In addition, the crystallinity (χ_c) of the copolymer could be calculated with the following formula:

$$\chi_c = \Delta H_f / \Delta H_f * \times 100\%$$

where ΔH_f is the endothermic peak area of the sample and ΔH_f^* (ca. 104 J/g for PVDF) is the endothermic peak area of the sample with 100% crystallinity.[30,33,34] Table I presents the data calculated

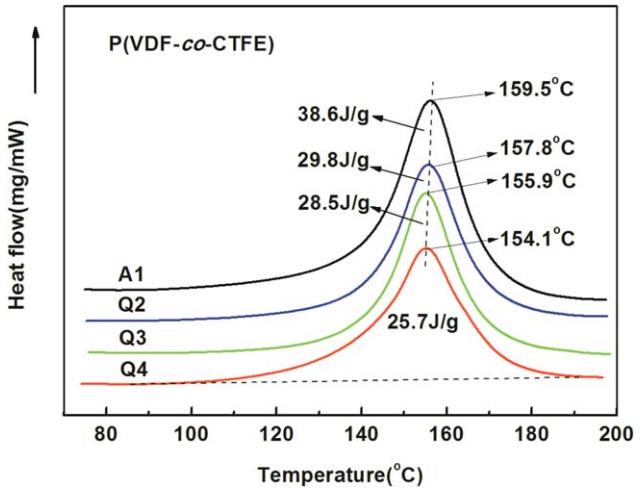

Figure 2. Differential scanning calorimetry curves of various treated P(VDF-*co*-CTFE) copolymers. [Color figure can be viewed in the online issue, which is available at wileyonlinelibrary.com.]

from the differential scanning calorimetry curves. As the quenching temperature decreased, the crystallinity of the P(VDF-*co*-CTFE) films dropped from 37.1% (A1) to less than 24.7% (Q4).

It is known that the formula $U_e = \int EdD$ is often used to calculate the discharged energy density of the nonlinear polymer, where E is usually known as E_b in calculating the largest U_e and D is the electric displacement at E_b. Interestingly, the low crystallinity of polymer favored a high E_b,[35] as was demonstrated by Fröhlich.[22,23] According to his calculation, the principal mechanism of electrical breakdown in a solid polymer consists of electronic breakdown, electromechanical breakdown, thermal breakdown, and gas-discharge breakdown. Under the glass-transition point, electronic breakdown is the predominant factor in destroying the polymer film. To express it, the collective electron approximated electrical breakdown theory depending on the amorphous phase was proposed, where E_b is determined by the depth of the shallow electronic energy level (ΔV), as shown in Figure 3. In the energy-level scheme, the conduction electron is derived from donor impurity levels lying deep ($V = 1$ eV or more) in the forbidden zone. Meanwhile, a set of shallow trap electrons spread below the conduction-band edge ($\Delta V < V$). If the volume of electrons in the conduction band, shallow trap, and deep trap are sufficient, these electrons transitions are expected to keep a balance in a strong applied E at a temperature above the lattice temperature of the solid. However, the balance of electron transitions from the shallow trap to the conduction trap could be destroyed if the energy of ΔV is sufficient. A great number of electron transitions will lead to the electrical breakdown of the polymer. Therefore, the electrical breakdown in an amorphous polymer is mainly dependent on ΔV, and the relation of E_b and ΔV is given by Fröhlich, as illustrated in the following formula:[22,36]

$$E_b \propto e^{\Delta V/4kT_0}$$

where T_0 is the lattice temperature determined by the testing temperature and k is a constant. It was believed that the increase in ΔV was due to the increasing interface between the amorphous phase and the spherical crystal grain in a low-temperature-quenched P(VDF-*co*-CTFE) film with depressed crystallinity.[23] As a result, the liquid-nitrogen-quenched copolymer film possessed a larger ΔV and a higher electric breakdown strength at a testing temperature of 25°C.

Moreover, the crystal grain sizes of the polymers processed at different temperature were compared by polarized optical microscopy micrographs at 1000×, as illustrated in Figure 4 and Table I. As the processing temperature decreased from 140 to −94°C, the diameter of crystal grain size decreased from about 60 to less than 5μm, and even the grain size of the liquid-nitrogen-quenched sample could not be detected and is not presented in the micrographs. Moreover, the spherical crystal grains in the Q2 and Q3 samples turned into lamellar crystals; this indicated that low-temperature quenching prevented the crystal core from growing into a large spherical crystal grain.

According to Fröhlich's electronic breakdown theory, the relationship of E_b to the diameter of the spherical crystal grain in the semicrystalline polymer could be described with eq. (1):[22]

$$E_b = A[\sqrt{(D_{cg}-d)^2+1\times10^{-10}}-(D_{cg}-d)]+E_0 \quad (1)$$

where A is a constant determined by the characteristics of the material and the test circumstances, D_{cg} is the diameter of the crystal grain in the polymer, d is the thickness of the film, and E_0 is the breakdown electric field in the case of $D_{cg} \geq d$. D_{cg} of

Table I. Crystalline Properties of the P(VDF-*co*-CTFE) Samples

Sample	Quenching or annealing temperature (°C)	Melting temperature (°C)[a]	ΔH_f (J/g)[a]	χ_c (%)	Diameter of crystal grain (μm)[b]	E_b (MV/m)[c]	E_f MV/m)[d]
A1	140	159.5	38.6	37.1	~60	228.7	212
Q1	25	157.8	31.2	30.1	~25	337.3	307
Q2	0	155.9	29.8	28.7	~10	397.5	440
Q3	−94	154.9	28.5	27.4	~5	471.4	530
Q4	−195.8	154.1	25.7	24.7	invisible	530	625

[a] From differential scanning calorimetry.
[b] Average diameter of the spherical crystal grain measured with polarized optical microscopy.
[c] Average test results of approximately 10 repetitions.
[d] Calculated value from eq. (1).

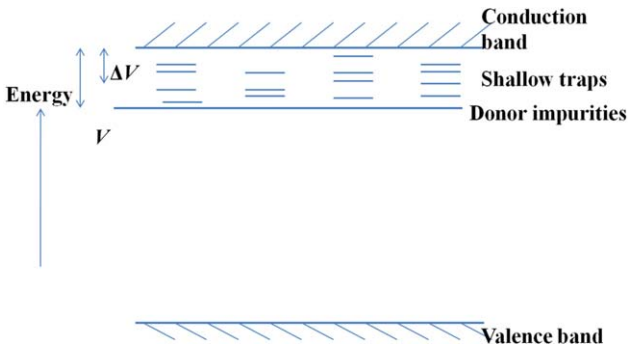

Figure 3. Model energy-level scheme for a polymer. [Color figure can be viewed in the online issue, which is available at wileyonlinelibrary.com.]

the A1 film was about 60 μm, as presented in Figure 4 and Table I; this was much higher than d (ca. 20 μm). Apparently, A1 with a large crystal grain size possessed a low E_b ($\sim E_0$). As the processing temperature was reduced, E_b increased as D_{cg} decreased, and a high average E_b of 530 MV/m was obtained in the Q4 sample. With E_b, the fitted values of A and E_0 were about 100 MV/m^2 and 200 MV/m, respectively, and the calculated E_f, depending on eq. (1), is listed in Table I. The fitted values illustrate that the small crystal grain diameter was responsible for the high E_b of the P(VDF-*co*-CTFE) films as well.

Dielectric Properties

In addition to E_b, ε_r is well known to be very essential to the energy storage polymer.[7–10] Figure 5 presents the dielectric response of the P(VDF-*co*-CTFE) films quenched at various temperatures as a function of the frequency from 50 Hz to 100 MHz. Apparently, the ε_r values of all of the samples decreased as the frequency increased; this coincided with the earlier reports for their dielectric relaxation and nonlinear nature.[11–15] We also notified that Q4, with a greater microcrystal phase, possessed a larger ε_r than the other samples in the low-frequency range from 100 Hz to 20 kHz. This may have been due to the large amount of interfacial regions formed during the quenching of the sample, where a lot of small crystalline regions are susceptible to the excitation of external E.[37] As a result, a high ε_r of 13.9 could be obtained in the liquid-nitrogen-quenched film at a frequency of 50 Hz; this was higher than that of the annealed sample ($\sim$12.5). As the test frequency was increased to 20 kHz, the dipole moment and the chain segmental motion could not follow the switching frequency of E any more, and their contribution to ε_r dropped immediately. Therefore, the dielectric loss (tan δ) increased with the frequency, and a loss peak appeared at a frequency about 5 MHz. Apparently, low-temperature quenching favored a high ε_r by reducing the crystal grain size while increasing the interfacial polarization of the P(VDF-*co*-CTFE) film.

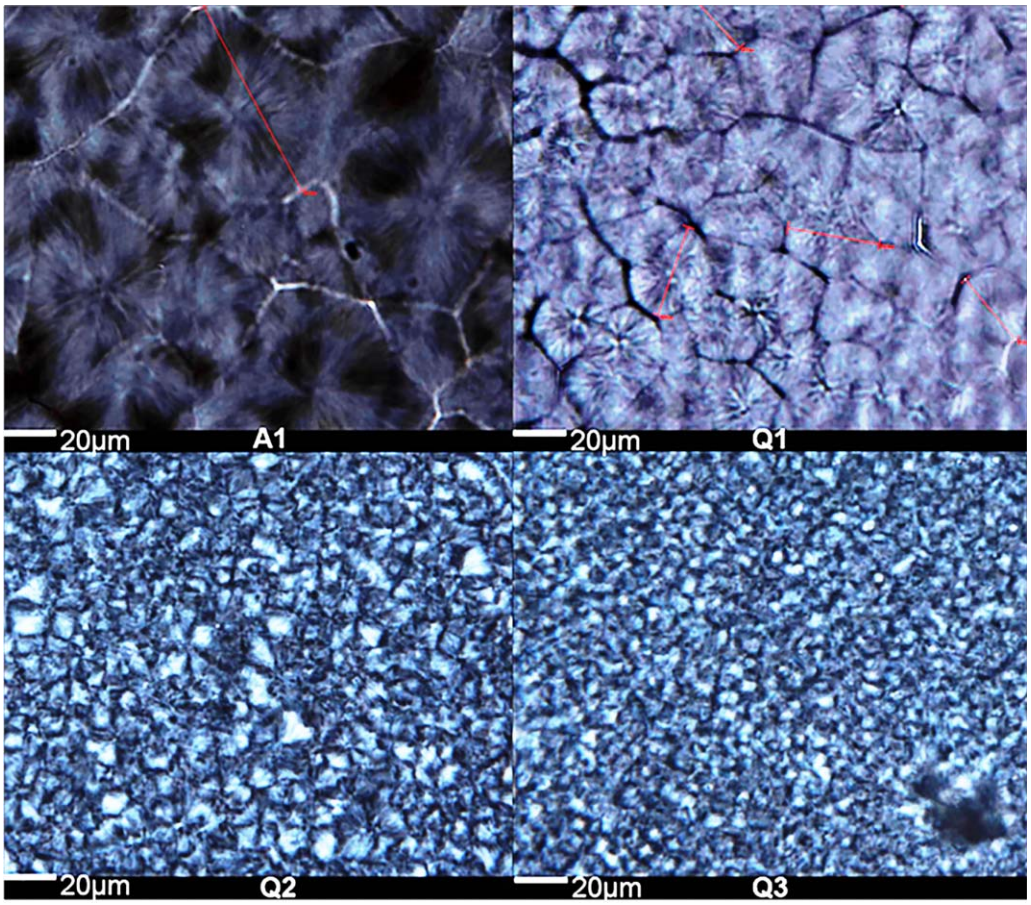

Figure 4. Polarized optical microscopy graphics of various treated P(VDF-*co*-CTFE) copolymers. [Color figure can be viewed in the online issue, which is available at wileyonlinelibrary.com.]

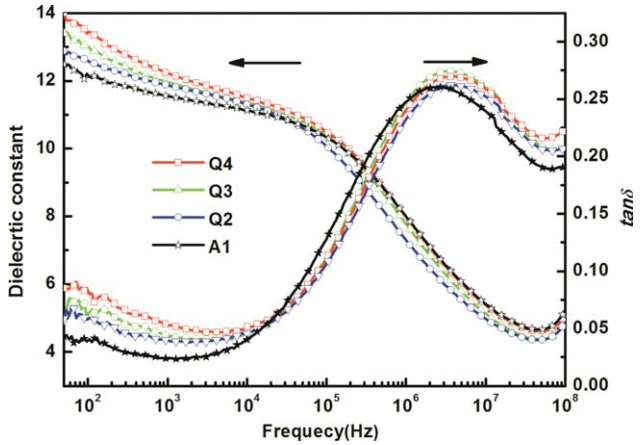

Figure 5. Dielectric properties of the copolymers treated at various temperatures as a function of the frequency measured at room temperature. [Color figure can be viewed in the online issue, which is available at wileyonlinelibrary.com.]

Figure 6 shows the temperature dependence of ε_r and tan δ of different P(VDF-*co*-CTFE) films at various frequencies. The ε_r values of all of the samples increased as the frequency decreased; this is expressed in Figure 5. Compared to A1, Q2, and Q3, Q4 also showed a higher ε_r at the same frequency and temperature. Above 100°C, both ε_r and tan δ showed an apparent enhancement as the temperature increased at a low frequency, and the weak peak (~120°C), which is known as the *premelting point,* of ε_r was found in all of the samples.[38,39] Because the crystallizing process of the quenching sample was so fast that the chain segments could not adjust themselves to optimized conformation, this left a lot of imperfections and defects in the small broken crystals in the interfacial regions. The defects reduced the activation energy of the chain segmental motion, and therefore, premelting occurred at a lower temperature for the quenched samples. Consequently, the onsets of the tan δ peak shifted toward lower temperatures as the temperature of the quenching bath dropped. As the frequency increased, the contributions of interfacial polarization were depressed, and the ε_r values of all of the samples decreased accordingly. Furthermore, near the melting point, peaks of tan δ appeared in the Q2, Q3, and Q4 samples; these were the melting points related to the crystallinity and crystal grain size of the α phase. As expected, a loss peak could not be found under 160°C in the A1 sample with its perfect, large crystalline region.

D Properties and Loss

To prove the effect of the depressed crystallinity on the displacement at high electric strength, *D–E* loops of the different samples at 200 MV/m are presented in Figure 7. Because of its low

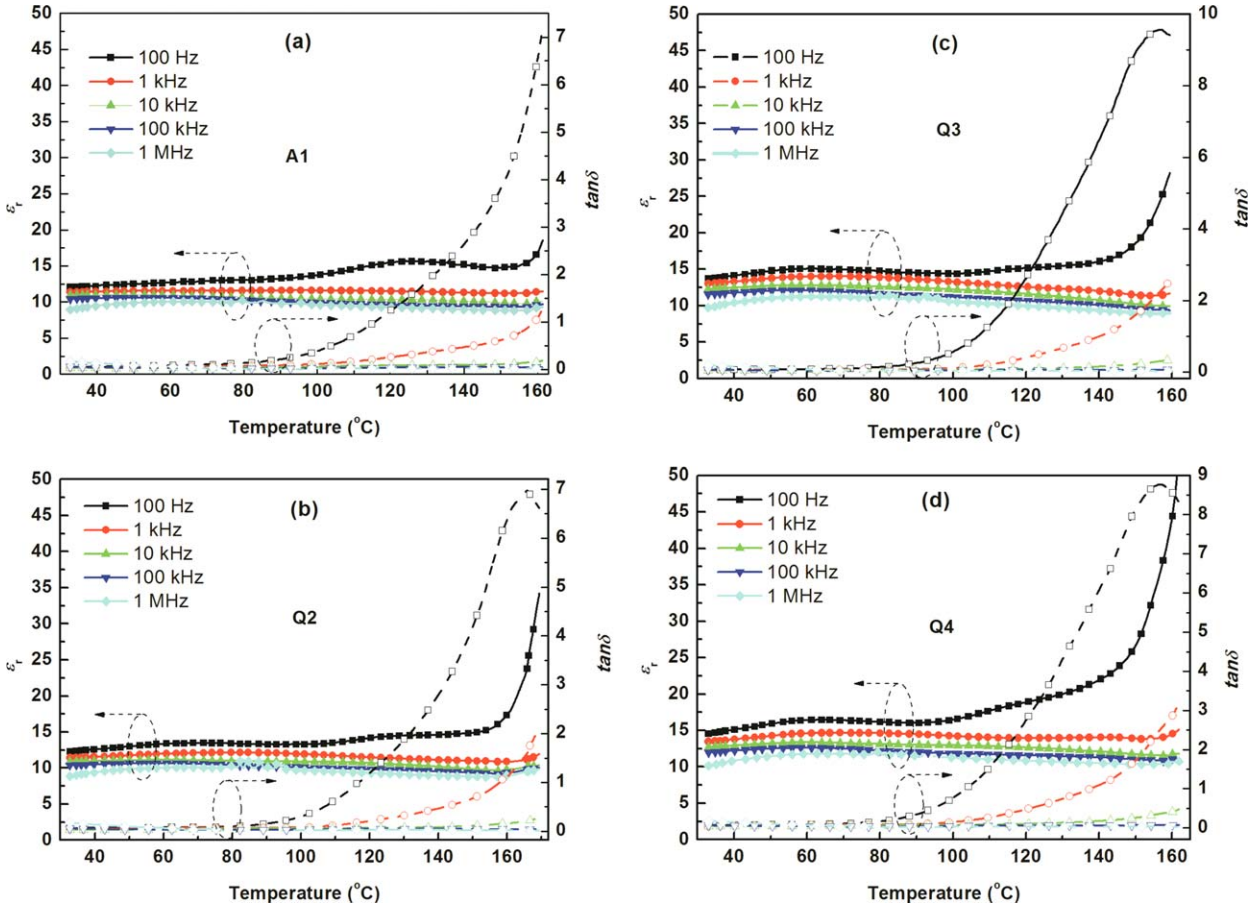

Figure 6. Dielectric properties as a function of the temperature for different samples: (a) A1, (b) Q2, (c) Q3, and (d) Q4. [Color figure can be viewed in the online issue, which is available at wileyonlinelibrary.com.]

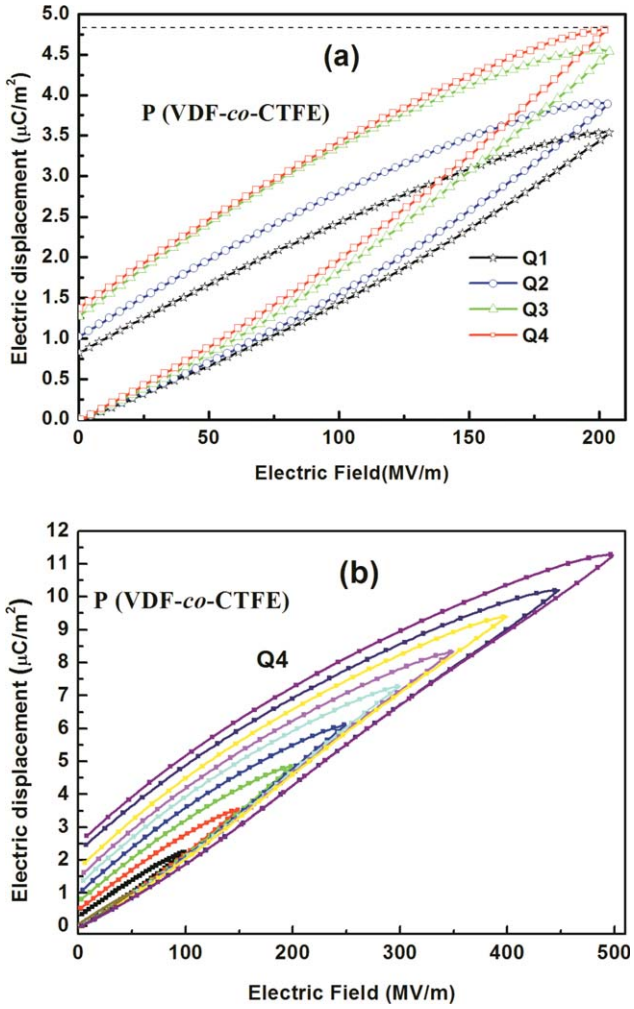

Figure 7. Unipolar D–E loops of the P(VDF-*co*-CTFE) copolymers: (a) differently treated samples at 200 MV/m and (b) liquid-nitrogen-quenched samples at various *E*s. [Color figure can be viewed in the online issue, which is available at wileyonlinelibrary.com.]

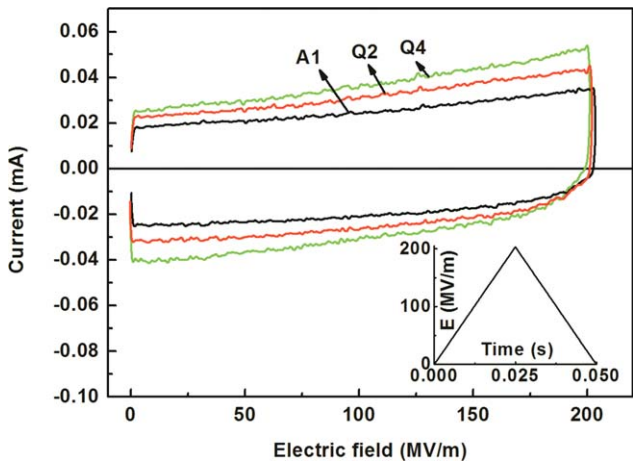

Figure 8. *I* values as the function of *E* for different samples. [Color figure can be viewed in the online issue, which is available at wileyonlinelibrary.com.]

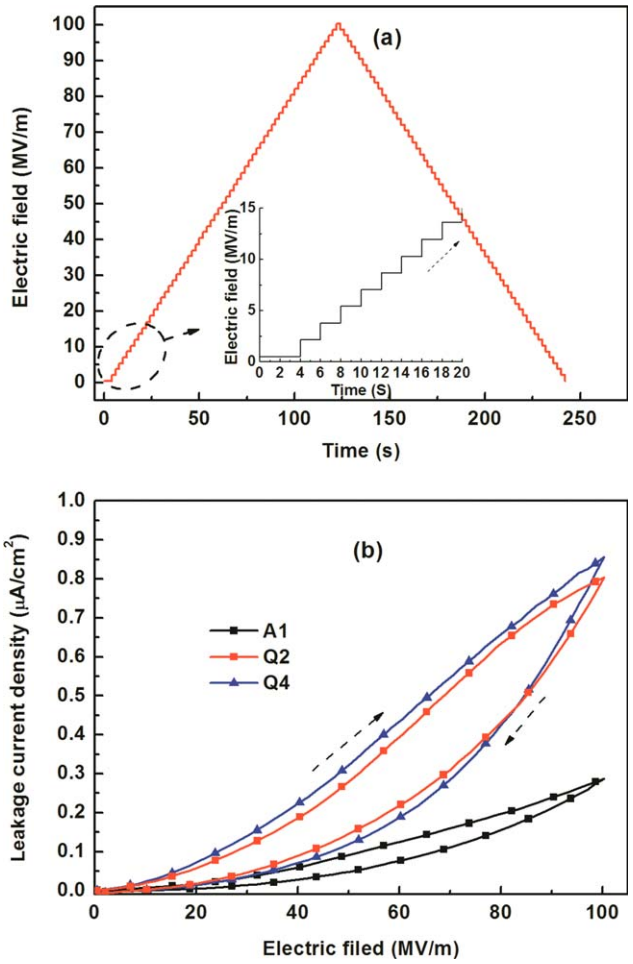

Figure 9. Leakage current density of different samples: (a) staircase wave of the applied *E* at a 2-s interval and (b) leakage current density as a function of *E* with the staircase wave. [Color figure can be viewed in the online issue, which is available at wileyonlinelibrary.com.]

crystallinity and crystal grain size,[24] Q4 possessed a large maximum displacement (D_m) and remnant displacement (D_r); this may have been due to more space charge polarization and dipole switching as *E* increased. Figure 7(b) shows the unipolar *D*–*E* hysteresis curves of Q4 as a function of *E*, and both D_m and D_r were enhanced with increasing *E*. As a result, a favorable D_m of 11.2 μC/cm^2 was obtained in the liquid-nitrogen-quenched sample at 500 MV/m.

At a high *E*, interfacial polarization was caused by the accumulation of free charge, which usually occurs in the interface of different crystal planes, phase boundaries, lattice deformations, defects, and impurities at a rather low frequency. In the low-temperature-quenched P(VDF-*co*-CTFE) film, space charge polarization may have been caused by the interface of the crystal and amorphous phases and even the defects of the inner crystal phase. To illustrate the contribution of space charges to *D*, we present *I* as a function of *E* (*I*–*E* curves replace *I*–*V* curves) at a definite thickness of 20 μm of A1, Q2, and Q4, as shown in Figure 8. The *I*–*E* curves showed an apparent parallelogram shape in the periodic *E* with a triangular wave at a frequency of 10 Hz; this was different from the rectangle shape of

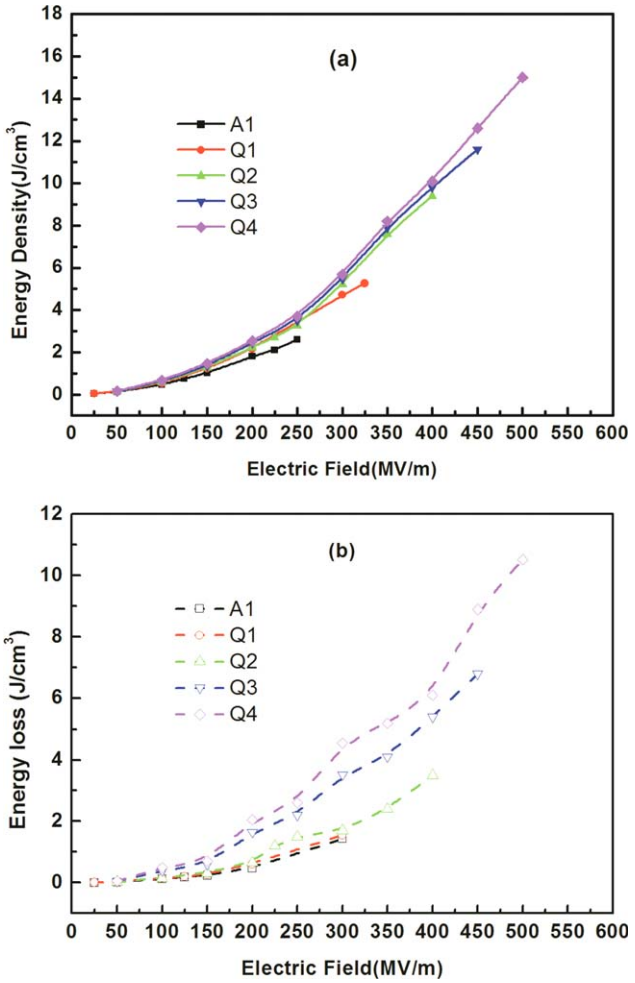

Figure 10. Discharged energy density and loss of different samples: (a) discharged energy density and (b) energy loss. [Color figure can be viewed in the online issue, which is available at wileyonlinelibrary.com.]

a standard capacitor. Compared to A1 and Q2, Q4 possessed a high I and a large capacitance ability, as indicated as in the following equation:

$$I = C^{du}/_{dt}$$

where du/dt is a constant that refers to the rate of change of voltage with time. In the ascent stage, du/dt is positive, and I of Q4 increased from 0.025 to 0.05 mA as E increased to 200 MV/m with increasing conduction of the space charges. In contrast, in the descent stage, du/dt turned negative abruptly, and the I should have been a negative value between −0.025 and −0.05 mA. However, when affected by the space charge polarization, the reversed I only reached near zero, and then it increased as E decreased and dropped to −0.04 mA. Figure 9 also presents the leakage current density as the function of unipolar E with increasing staircase wave at a ratio of 1.67 MV/m with a 2 s interval. In the ascent stage, the leakage current densities of A1, Q2, and Q4 increased gradually; this indicated that the increasing space charges migrated with the direction of E. Apparently, this migration may have contributed to D, and therefore, a large increase rate and a high value of the leakage current density (0.9 μA/cm^3) were obtained in the Q4 sample. As E decreased, the leakage current density decreased accordingly. In this cycle shown in Figure 9, the leakage current density of the ascent stage was larger than that of the descent stage, and the charge–discharge process was a sharp, horn-shaped curve. This illustrated that the space charges decreased as E decreased. Consequently, in addition to the contribution of dipoles, the leakage current density may have resulted in the high D at high E.

Discharged Energy Density and Loss

The discharged energy density and loss of the copolymers under various Es were calculated from the unipolar D–E hysteresis loops in Figure 7.[8] As shown in Figure 10(a), the discharged energy density increased with E with increasing dipole switching. Meanwhile, the energy density of Q4 increased faster than for the other samples, and a large discharged energy density of 15.32 J/cm^3 was obtained at an E about 530 MV/m. However, Figure 10(b) shows that Q4 possessed a higher energy loss than the other samples; this was mainly attributed to the dipole relaxation and the large conduction loss caused by space charges. Nevertheless, low-temperature quenching effectively improved the energy storage capability of the P(VDF-*co*-CTFE) film at different DC strengths. For high-pulse-capacitor application purposes, the large energy density provided a more practical value at high E.

CONCLUSIONS

In conclusion, the effect of the thermal treatment on the dielectric, displacement, and energy storage properties of P(VDF-*co*-CTFE) (91/9 mol %) was investigated. The results indicate that quenching at a lower temperature depressed the crystallinity from 38.9 to 27.6% and reduced the crystal grain size from about 60 to less than 5 μm of that of the copolymer. As a result, ε_r increased slightly at a low frequency because of the response of dipoles and interfacial polarization. It was proven that the improvement in E_b and the increase in polarization in the low-temperature-quenched polymer film was caused by the low crystallinity and small crystal grain size; this was expressed well by Fröhlich theory. By introducing the space charge contribution, the D of film quenched at lower temperatures was dramatically enhanced. In addition to chemical (i.e., copolymerization) and mechanical (i.e., stretching) fabrication, this was an effective way to improve the electric properties of this PVDF-based copolymer.

ACKNOWLEDGMENTS

This work was supported by the National Natural Science Foundation of China (contract grant number 51103115) and the Nature Science Foundation of the Shaanxi Provincial Education Office (contract grant number 2015JM5155).

REFERENCES

1. Tan, Q.; Irwin, P.; Cao, Y. *IEEJ Trans. Fundam. Mater.* **2006**, *126*, 1153.
2. Sarjeant, W. J. *IEEE Trans. Plasma Sci.* **1990**, *25*, 861.
3. Sarjeant, W. J.; Zirnheld, J.; MacDougall, F. W. *IEEE Trans. Plasma Sci.* **1998**, *26*, 1368.

4. Nalwa, H. S. Ferroelectric Polymers: Chemistry, Physics, and Applications; Marcel Dekker: New York, **1995**.
5. Zhou, X.; Chu, B. J.; Neese, B.; Lin, M.; Zhang, Q. M. *IEEE Trans. Dielectr. Electr. Insul.* **2007**, *14*, 1133.
6. Zhang, Q. M.; Bharti, V.; Zhao, X. *Science* **1998**, *280*, 2101.
7. Chu, B. J.; Zhou, X.; Ren, K. L.; Neese, B.; Lin, M. R.; Wang, Q.; Bauer, F.; Zhang, Q. M. *Science* **2006**, *313*, 334.
8. Zhang, Z. C.; Chung, T. C. M. *Macromolecules* **2007**, *40*, 783.
9. Li, W. J.; Zhang, Z. C.; Meng, Q. J.; Zheng, Y. S.; Xia, W. M.; Xu, Z. *Appl. Phys. Lett.* **2010**, *96*, 192905.
10. Lu, Y. Y.; Claude, J.; Neese, B.; Zhang, Q. M.; Wang, Q. *J. Am. Chem. Soc.* **2006**, *128*, 8120.
11. Meng, Q. J.; Zhang, Z. C.; Chung, T. C. M. *Polymer* **2009**, *50*, 707.
12. Zhao, C. Q.; Guo, M. T.; Lu, Y. Y.; Wang, Q. *Macromol. Symp.* **2009**, *279*, 52.
13. Zhang, Z. C.; Chung, T. C. M. *Macromolecules* **2007**, *40*, 9391.
14. Wang, Z. M.; Zhang, Z. C.; Chung, T. C. M. *Macromolecules* **2006**, *39*, 4268.
15. Lu, Y. Y.; Claude, J.; Zhang, Q. M.; Wang, Q. *Macromolecules* **2006**, *39*, 6962.
16. Guan, F. X.; Yuan, Z. Z.; Shu, E. W.; Zhu, L. *Appl. Phys. Lett.* **2009**, *94*, 052907.
17. Guan, F. X.; Pan, J. L.; Wang, J.; Wang, Q.; Zhu, L. *Macromolecules* **2010**, *43*, 384.
18. Zhu, L.; Wang, Q. *Macromolecules* **2012**, *45*, 2937.
19. Xu, H. S.; Shen, D.; Zhang, Q. M. *Polymer* **2007**, *48*, 2124.
20. Zhang, Z. C.; Wang, Z. M.; Chung, T. C. M. *Macromolecules* **2007**, *40*, 5235.
21. Chung, T. C.; Petchsuk, A. *Macromolecules* **2002**, *35*, 7678.
22. Fröhlich, H. Theory of Dielectrics; Oxford University Press: London, **1947**; p 90.
23. Ieda, M. *IEEE Trans. Insul.* **1980**, *EI-15*, 206.
24. Xia, W. M.; Xu, Z.; Wen, F.; Li, W. J.; Zhang, Z. C. *Appl. Phys. Lett.* **2010**, *97*(22), 222905.
25. Davies, G. R.; Singh, H. *Polymer* **1979**, *20*, 772.
26. Naegele, D.; Yoon, D. Y.; Broadhurst, M. G. *Macromolecules* **1978**, *11*, 1197.
27. Lovinger, A. J. *Macromolecules* **1982**, *15*, 40.
28. Lovinger, A. J.; Davies, G. T.; Furukawa, T. *Macromolecules* **1982**, *15*, 323.
29. Warren, B. E. X-Ray Diffraction; Dover: New York, **1990**.
30. Klein, R. J.; Runt, J.; Zhang, Q. M. *Macromolecules* **2003**, *36*, 7223.
31. Xia, W. M.; Xu, Z.; Zhang, Q. P.; Zhang, Z. C. *J. Polym. Sci. Part B: Polym. Phys.* **2012**, *50*, 1271.
32. Meng, Q. J.; Li, W. J.; Zheng, Y. S.; Zhang, Z. C. *J. Appl. Polym. Sci.* **2010**, *116*, 2674.
33. Xia, F.; Wang, Y. K.; Li, H.; Huang, C.; Ma, Y.; Zhang, Q. M.; Cheng, Z. Y. *J. Polym. Sci. Part B: Polym. Phys.* **2003**, *41*, 797.
34. Prest, W. M., Jr.; Luca, D. J. *J. Appl. Phys.* **1978**, *49*, 5042.
35. von Hippel, A. R.; Maurer, R. *J. Phys. Rev.* **1941**, *59*, 820.
36. Blythe, A. R. Electrical Properties of Polymers; Cambridge University Press: London, **1979**; p 140.
37. Chen, X. Z.; Li, X. Y.; Qian, X. S.; Wu, S.; Lu, S. G.; Gu, H. M.; Lin, M. R.; Shen, Q. D.; Zhang, Q. M. *Polymer* **2013**, *54*, 2373.
38. Yang, L. Y.; Allahyarov, E.; Guan, F. X.; Zhu, L. *Macromolecules* **2013**, *46*, 9698.
39. Yang, L. Y.; Li, X. Y.; Allahyarov, E.; Taylor, P. L.; Zhang, Q. M.; Zhu, L. *Polymer* **2013**, *54*, 1709.